# Journal of Materials Chemistry C

Accepted Manuscript


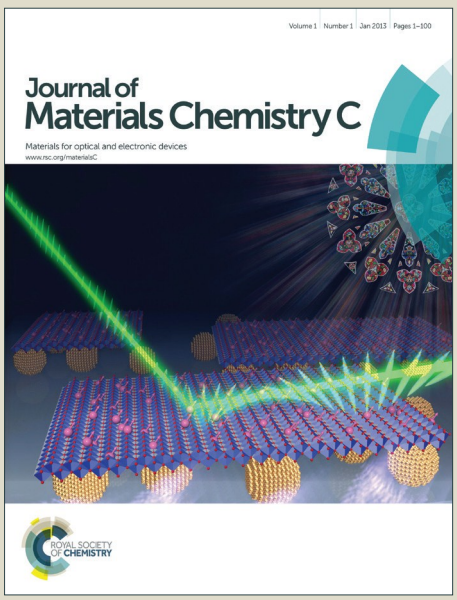





ROYAL SOCIETY OF CHEMISTRY

www.rsc.org/materialsC

Journal Name

ARTICLE

# Synthesis of Copper Nanoparticles within the Interlayer Space of Titania Nanosheet Transparent Films

Received 00th January 20xx,
Accepted 00th January 20xx

DOI: 10.1039/x0xx00000x

www.rsc.org/

Kazuhisa Sasaki,[a] Kazuki Matsubara,[a] Shiori Kawamura,[a] Kenji Saito,[a] Masayuki Yagi,[a] Wataru Norimatsu,[b] Ryo Sasai,[c] and Tatsuto Yui[a]*

We report the first *in situ* synthesis of copper nanoparticles (CuNPs) within the interlayer space of inorganic layered compounds (titania nanosheet films) through the following steps. A sintered titania nanosheet (s-TNS) film was synthesised, forming a transparent, layered semiconductor film (~2 μm thick). A considerable amount of copper ions (ca. 68% relative to the cation exchange capacity of TNS) were intercalated in the s-TNS using the methyl viologen-containing s-TNS as an intermediate. The resultant copper-containing s-TNS (TNS/$Cu^{2+}$) film was treated with an aqueous solution of $NaBH_4$,resulting in a colour change. Extinction spectra of $NaBH_4$-treated films exhibited a wide extinction band at $\lambda_{max}$ (the extinction band maximum) = 683 nm. The spectral shapes and $\lambda_{max}$ were similar to those for copper nanoparticles on $TiO_2$ surfaces. Transmission electron microscopy analysis demonstrated the wide distribution of electron dense particles on the titania sheet of $NaBH_4$-treated TNS/$Cu^{2+}$. XRD analysis and absorption/extinction analysis with different amounts of TNS suggest that CuNPs were formed within the interlayer space rather than the surface of TNS through $NaBH_4$ treatment. Repeatable oxidation and reduction behaviour, i.e. colouration and decolouration cycles of the copper species within TNS films, were investigated.

## Introduction

Many inorganic layered materials have a two-dimensional, wide (typically several hundred $m^2\ g^{-1}$) and expandable layered structure of stacked inorganic sheets with a thickness of only a few angstroms.[1-4] Their expandable properties enable the incorporation of various chemical species, typically ionic molecules, into their interlayer space with varying layer distances. The reversible insertion of guest species into layered spaces is known as intercalation. In many cases, the intercalated species form a regularly aligned structure through interactions between the layer surface and the intercalated chemical species.[2-7] Thus, such two-dimensionally ordered systems are very interesting as molecular vessels, reaction fields and templates for the synthesis of various chemical species.[1-3] Among these, layered metal oxide semiconductors (LMOSs) have been extensively investigated owing to their intercalation, semiconducting and photocatalytic properties.[1-3] In particular, layered titanium oxides and their complete exfoliated materials (titania nanosheet; TNS) were widely investigated due to their unique chemical and physical properties.[8-13] Photochemical and photocatalytic properties of TNS thin films[12] constructed from electrophoretic deposition,[13] drop-casting method,[8-11] Langmuir-Blodgett (LB) deposition[14] or layer-by-layer (LbL) deposition[15, 16] have been widely investigated. Synthesis of optically transparent TNS films with effective thicknesses is important from the standpoint of photochemical and photocatalytic investigations.

Noble metal nanoparticles (MNPs) such as gold, silver and copper exhibit characteristic light absorption and scattering due to their localised surface plasmon resonance (LSPR).[17-20] Thus, NPs can be used in various photochemical and optical applications, such as light harvesting,[21] fluorescence enhancement[22] and photoelectric devices.[23] In addition, combination of MNPs and metal oxide semiconductors (MOSs), such as $TiO_2$, can be applied to new types of photocatalysis,[24, 25] such as hydrogen reduction,[26] water oxidation,[27, 28] water splitting,[29] $CO_2$ reduction,[30, 31] etc.[31-34] However, most semiconductor particles have low surface areas, resulting in minimal MNPs on the semiconductor surface. While LMOSs can be used in place of MOS particles, it is expected that relatively large amounts of MNPs are hybridised with the semiconductors.

Hybridisation of MNPs and inorganic layered compounds has been reported; however, most of these procedures require MNP synthesis prior to being hybridised with inorganic layered compounds.[35-37] As an exception, Sasaki et al. reported the synthesis of $Ag^+$ and TNS films through LbL techniques and

[a] Department of Material Science and Technology, Faculty of Engineering, and Center for Transdisciplinary Research, Niigata University, 8050 Ikarashi–2, Niigata 950–2181, Japan. E–mail: ttt_yui@mac.com
[b] Department of Applied Chemistry, Graduate School of Engineering, Nagoya University, Furo–cho, Chikusa–ku, Nagoya–shi, Aichi–ken, 464–8603, Japan
[c] Department of Physics and Materials Science, Interdisciplinary Graduate School of Science and Engineering, Shimane University, 1060, Nishi–kawatsu–cho, 690–8504 Matsue, Japan

† Footnotes relating to the title and/or authors should appear here.
Electronic Supplementary Information (ESI) available: XRD, SEM, EDS, TEM, ED, and absorption/extinction analyses. See DOI: 10.1039/x0xx00000x

synthesis of AgNP within the TNS interlayers using the photocatalytic properties of TNS.[15] However, not only does the LbL technique require complicated procedures and significant effort but the resultant film is also very thin (approximately 20 layers of single TNS sheets).[15] Here, we report the synthesis of a transparent TNS film, metal cation-containing TNS film and MNP-containing TNS film without complex procedures. Typically, the *in situ* reduction of metal cations within the TNS film through the use of a reductant has not yet been reported. As such, we focused on copper nanoparticles (CuNPs) or copper oxide nanoparticles as representative nanoparticles, as oxide-derived nanocrystalline copper is used as an efficient electrocatalyst for the transformation of carbon monoxide to liquid fuel.[38-40] Herein, we report the first ever synthesis of copper and copper oxide nanoparticles within the interlayer space of inorganic layered materials (transparent TNS films) through simple processes.

## Experimental Section

### Materials

Methyl viologen dichloride ($MV^{2+}$ $2Cl^-$; 98%, Aldrich), tetrabutylammonium hydroxide ($TBA^+$ $OH^-$; 40% in water, TCI), anatase titanium dioxide ($TiO_2$, ST-01, Ishihara Sangyo Ltd.), cesium carbonate ($Cs_2CO_3$; 99.99%, Kanto Chemical Co., Inc.), and poly(vinyl alcohol) (PVA; $M_w$ ~ 88,000, Kanto Chemical Co., Inc.), hydrochloric acid (HCl, Junsei Chemical Co., Ltd.), sodium hydroxide (NaOH, Junsei Chemical Co., Ltd.), copper(II) nitrate trihydrate ($Cu(NO_3)_2$, Kanto Chemical Co., Inc.), sodium tetrahydroborate ($NaBH_4$, Junsei Chemical Co., Ltd.) were used without further purification. Ultrapure water (18.2 MΩ $cm^{-1}$) used in this study was produced by a Milli-Q water purification system (Direct-Q® 3UV, Millipore).

### Synthesis of TNS colloidal suspensions

Titania nanosheets (TNS; $Ti_{0.91}O_2$) were prepared according to the well-established procedure reported previously.[41, 42] A stoichiometric mixture of $Cs_2CO_3$ and $TiO_2$ (ST-01) was calcined at 800 °C for 20 h to form the starting material of layered cesium titanates, $Cs_{0.7}Ti_{1.825}\square_{0.175}O_4$ (□: vacancy at Ti octahedral site).[41] The product was repeatedly treated with 1 mol $L^{-1}$ HCl aqueous solution to convert them into protonated forms of $H_{0.7}Ti_{1.825}\square_{0.175}O_4{\cdot}H_2O$. The obtained protonated powder was shaken vigorously with 100 mL of a $1.7 \times 10^{-2}$ mol $L^{-1}$ $TBA^+$ $OH^-$ aqueous solution for about 2 weeks at ambient temperature. The resulting opalescent suspension (1.6 g $L^{-1}$, pH = 11 ~ 12) contained exfoliated titania nanosheets.

### Synthesis of TNS films

**Cast film of TNS (c-TNS).** Pyrex glass substrates (~20 × 20 $mm^2$) were precleaned through successive ultrasonic treatments in 1 mol $L^{-1}$ aqueous NaOH and ultrapure water for >1 h each, rinsed with ultrapure water and dried at room temperature. The colloidal suspension of TNS was cast on the glass substrate in 300 μL aliquots and dried in air at 60 °C for >2 h.

**Sintered TNS film (s-TNS).** The obtained c-TNS film was sintered in air at 500 °C for 3 h (heating from 25 to 500 °C at a rate of 6.8 °C $min^{-1}$) to achieve thermal fixation of the TNS components on the glass substrate.

**$MV^{2+}$ Intercalated TNS films (TNS/$MV^{2+}$).** An s-TNS film was immersed in an aqueous solution of methyl viologen ($MV^{2+}$) $2Cl^-$ ($2 \times 10^{-4}$ mol $L^{-1}$) for 7 h at room temperature, rinsed with ultrapure water and dried in air at 60 °C in the dark.

**$Cu^{2+}$ Intercalated TNS films (TNS/$Cu^{2+}$).** A TNS/$MV^{2+}$ film was immersed in an aqueous solution of $Cu(NO_3)_2$ (0.1 mol $L^{-1}$) for 24 h at room temperature, rinsed with ultrapure water and dried in air at room temperature in the dark.

**Synthesis of CuNP within the Interlayer Space of TNS films (TNS/CuNP).** A TNS/$Cu^{2+}$ film was immersed in an aqueous solution of $NaBH_4$ (0.1 mol $L^{-1}$) for 0.5 h at room temperature under dark conditions.

### Film Characterizations.

X-ray diffraction (XRD) analyses were carried out using a desktop X-ray diffractometer (MiniFlex II, Rigaku) with monochromatized Cu-Kα radiation (λ = 1.5405 Å), operated at 30 kV and 15 mA. Scanning electron microscope (SEM) images were taken using a JEOL JSM–6510LV operating at an accelerating voltage of 15 kV. EDS spectra were taken using a JED-2300. TEM images were taken using a Topcon EM-002B operating at an accelerating voltage of 200 kV. X-ray photoelectron spectra (XPS) were taken using a JPS-9000 XPS (JEOL) spectrometer with an Mg-Kα X-ray line (1254 eV). A multichannel photodetector (MCPD-3700, Otsuka Electronics) was employed to record UV-vis absorption spectra for the prepared samples.

## Results and Discussion

### Synthesis of transparent s-TNS films

The X-ray diffraction (XRD) profiles of the TNS cast (c-TNS) and sintered (s-TNS) films are shown in Figure S1. Three sharp characteristic peaks were observed for c-TNS at 2θ = 5.1, 10.2 and 15.2° with a layer distance of d(002) = 1.72 nm. Observation of three narrow series of reflection signals suggested that the TNS layers aligned in a relatively regular and parallel orientation to the substrate. The thickness of one layer of TNS sheet was reported to be 0.45 nm,[13] and thus the estimated clearance space (CLS) of c-TNS is 1.27 nm. This indicates that the tetrabutylammonium cation ($TBA^+$; molecular length ~1.1 nm) and water molecules (ca. 0.3 nm) were intercalated in the c-TNS layers in a monolayer fashion. The s-TNS film was prepared via sintering procedures from the c-TNS film, shifting the d(002) peak to a higher angle (2θ = 10.4° and d(002) = 0.85 nm). This d-value is slightly shorter than that for protonated, layered titanate ($H_{0.7}Ti_{1.825}\square_{0.175}O_4{\cdot}H_2O$, d = 0.94 nm), which is a precursor of TNS.[41, 42] This suggests that $TBA^+$ and water were removed by sintering treatment at 500 °C, with s-TNS potentially maintaining a layered structure similar to that of a protonated layered titanate.

Transmittance spectra of c-TNS and s-TNS, together with that of a $TiO_2$ film prepared from commercially available $TiO_2$ particles (ST-01) with poly(vinyl alcohol) (PVA) as a supporting regent, are shown in Figure 1A. ST-01 and PVA film (ST-

01/PVA) were less transparent at all wavelength regions (see Figure 1A, line a) due to the strong light scattering of $TiO_2$ particles on the substrate. The scanning electron microscopy (SEM) image clearly demonstrated that the ST-01/PVA film formed an uneven film structure with a wide distribution of film thickness (4–25 μm), causing strong light scattering (Figure S2a). In contrast, c-TNS exhibited relatively good transparency in the visible wavelength region and strong absorption in the UV region due to the band gap absorption of TNS. The s-TNS film demonstrated better transparency than the c-TNS film, as shown in Figure 1, as s-TNS possessed a flat and uniform film structure (ca. 2 μm thick, Figure S2b). Such good transparency enabled the measurement of the absorption spectra in the transmittance mode, allowing for use in various photochemical applications. The obtained s-TNS was soaked in pure water for 40 h without removal of any TNS film being observed; thus, s-TNS displayed good adherence to the glass substrate without the need for an assistant reagent such as a PVA.[8-11, 13]

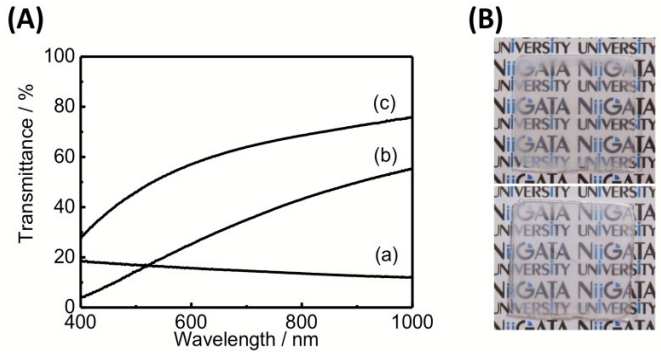


Figure 1. (A) Transmittance spectra of (a) ST-01/PVA, (b) c-TNS and (c) s-TNS films. (B) Photographs of c-TNS (top) and s-TNS films (bottom).

### Synthesis of TNS/$MV^{2+}$ and TNS/$Cu^{2+}$ films

The TNS/$MV^{2+}$ film was synthesised as a precursor[3, 10, 13, 43] for the TNS/$Cu^{2+}$ and TNS/CuNP films. The XRD profile of TNS/$MV^{2+}$ is shown in Figure 2A. Two peaks were observed at $2\theta$ = 7.9 and 15.6° (d(002) = 1.12 nm), and the CLS was estimated to be 0.67 nm. This suggests that $MV^{2+}$ (molecular size: ~1.3 × 0.4 nm[13]) were intercalated in the TNS layer in a nearly parallel fashion to the TNS layers.[13] When the TNS/$MV^{2+}$ film was soaked in a $Cu(NO_3)_2$ solution, the two peaks shifted to a higher angle region (Figure 2B), with the d(002) and CLS of TNS/$Cu^{2+}$ estimated to be 0.86 and 0.44 nm, respectively. This suggests that ion exchange from $MV^{2+}$ to $Cu^{2+}$ proceeded under the experimental conditions, as the ionic radius of $Cu^{2+}$ (0.074 nm[44]) was significantly smaller than that of $MV^{2+}$. Thus, we can conclude that $Cu^{2+}$ and water molecules exist within the interlayer space of TNS. Intercalation of copper species was estimated by EDS analysis, which provided clear signals for Ti and Cu. The atomic ratio of Ti:Cu was estimated to be 1:0.136±0.002, which corresponds to 68±9% relative to the cation exchange capacity (CEC) of TNS (see ESI). Based on these results, it was determined that considerable amounts of Cu species were intercalated in the TNS interlayers, with $Cu^{2+}$ potentially oriented as a bilayer structure.

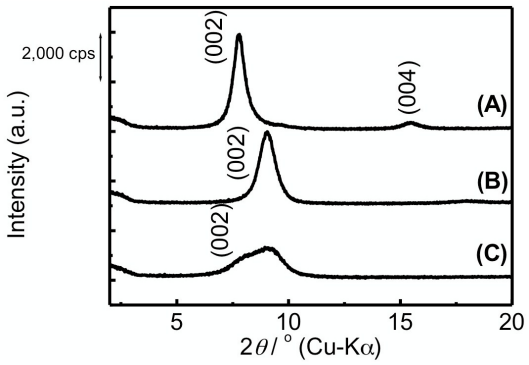


Figure 2. X-ray diffraction profiles of (A) TNS/$MV^{2+}$, (B) TNS/$Cu^{2+}$ and (C) $NaBH_4$-treated TNS/$Cu^{2+}$ films.

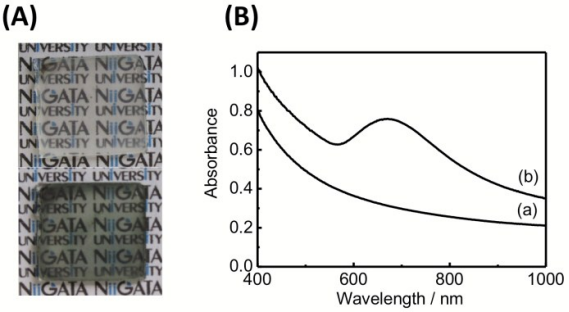


Figure 3. (A) Photograph of TNS/$Cu^{2+}$ (top) and $NaBH_4$-treated films (bottom). (B) Transmittance extinction spectra of (a) TNS/$Cu^{2+}$ and (b) $NaBH_4$-treated films.

### Synthesis of TNS/CuNP film

Upon treatment of the TNS/$Cu^{2+}$ film with $NaBH_4$ as a reductant, the colour of the film immediately changed from clear to metallic grey, as shown in Figure 3A. A new extinction band at $\lambda_{max}$ = 683 nm was observed upon treatment with $NaBH_4$, as shown in Figure 3B. The observed extinction band maximum was similar to that of the LSPR band of spherical copper nanoparticles on $TiO_2$,[45, 46] suggesting that Cu(0) nanoparticles formed within the interlayer space of TNS. EDS analysis (Figure S3 and Table S1) showed that 62±24% CEC of copper species were detected for the $NaBH_4$-treated film, suggesting that $Cu^{2+}$ and/or Cu(0) were not desorbed as a result of $NaBH_4$ treatment. Such a large standard deviation for copper implies non-uniform distribution of copper species within the interlayer space of TNS (Figure S4). The XRD profiles of TNS/$Cu^{2+}$ and $NaBH_4$-treated films are shown in Figures 2B and 2C, respectively. The characteristic d(002) = 0.95 nm signal was observed for the $NaBH_4$-treated film with a nearly identical peak position to that of the TNS/$Cu^{2+}$ film. However, the $NaBH_4$-treated film exhibited a broader XRD signal than that of TNS/$Cu^{2+}$, indicating that the layered stacking structure remained unchanged; however, the regular stacking structure became disordered upon $NaBH_4$ treatment.

For confirming the formations of the CuNPs within the interlayer space rather than the surface of TNS films, the relation between the amounts of TNS on the glass substrate and the CuNPs generated through $NaBH_4$ treatment was investigated. If the CuNPs are formed only on the surface of TNS films, the amounts of TNS and CuNPs should be independent. c-TNS films having different amounts of TNS on the glass substrate were prepared by varying the casted volume of TNS suspensions ($V$ = 150–900 μL). Similar procedures to those described in the experimental section were used to obtain TNS/$Cu^{2+}$ films from these various c-TNS films. The absorption intensities of TNS/$Cu^{2+}$ films at 380 nm, i.e. the band-edge absorption of TNS, were plotted against $V$, as shown in Figure S5. The absorption intensities of TNS monotonically increased with increasing $V$, indicating that the current procedures enabled deposition of various amounts of TNS on the glass substrate. Upon treatment of the obtained TNS/$Cu^{2+}$ films with $NaBH_4$, a characteristic extinction band at $\lambda_{max}$ = 680 nm appeared for all TNS/$Cu^{2+}$ films. The relations between the absorption intensities at 380 nm for TNS/$Cu^{2+}$ films as the intermediate and the extinction intensities at 680 nm for $NaBH_4$-treated TNS/$Cu^{2+}$ films are shown in Figure 4. The extinction intensities of CuNPs monotonically increased with increasing absorption intensities of TNS. This clearly indicates that a strong relation exists between the amounts of TNS and CuNPs generated, leading to the conclusion that CuNPs were formed in the interlayers rather than the surface of TNS films.

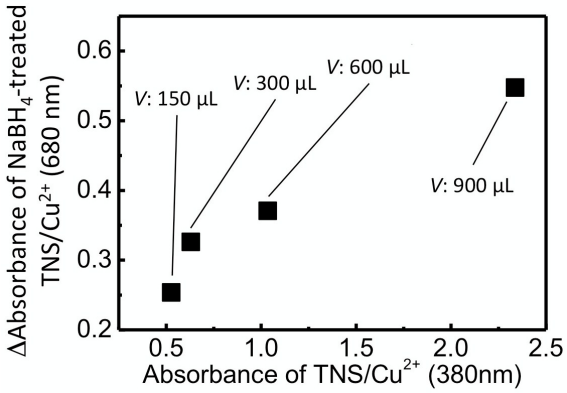


Figure 4. Relation between the absorption intensities at 380 nm for TNS/$Cu^{2+}$ films and the extinction intensities at 680 nm for $NaBH_4$-treated TNS/$Cu^{2+}$ films.

In general, the extinction spectral shape and $\lambda_{max}$ of CuNP are very sensitive to the particle shape and size,[29, 47] interparticle distance[48] and refractive index[49] of the surrounding media.[46, 50] Thus, particle shape and distribution of CuNPs within the interlayer space of TNS were analysed by transmission electron microscopy (TEM). The TEM image of s-TNS without copper species is shown in Figure S6, showing a smooth and uniform layered structure. The TEM image and electron diffraction (ED) pattern (Figure S7) were consistent with previous reports.[51, 52] In contrast, dark (i.e. heavier) dots with wide size and shape distributions (3–40 nm) were observed for the $NaBH_4$-treated TNS/$Cu^{2+}$ film (Figure 5A), implying the generation of copper nanoparticles through $NaBH_4$ treatment. TEM and ED analyses showed that a large part of these dots had an amorphous structure. However, characteristic lattice image corresponding to CuO was observed at dark dots, as very minor species (Figure S8). These results may conclude that the dark dots are composed of copper species. The dark dot was sandwiched by TNS layer (Figure 5(B)), thus, this clearly indicate that copper species were intercalated and accommodated within the inter layer of TNS. Characteristic XPS signal was observed at 933 eV (Cu $2p_{3/2}$) that correspond to copper species for $NaBH_4$-treated TNS/$Cu^{2+}$ films. In contrast, no signals were detected for c-TNS films in this region (Figure S9). However, exact chemical structure of copper specie was not identified due to our apparatus resolution (Cu: 932.5 eV, $Cu_2O$: 933.1 eV, and CuO: 933.9 eV).[53] Therefore, the chemical structure of these particles, i.e. Cu(0), $Cu_2O$ and CuO, or their core-shell structures have not yet been identified. As described below, the copper species in TNS were easily oxidised even in the film state; thus, once generated, Cu(0) nanoparticles may be oxidised during the sample preparation for TEM and XPS analysis.

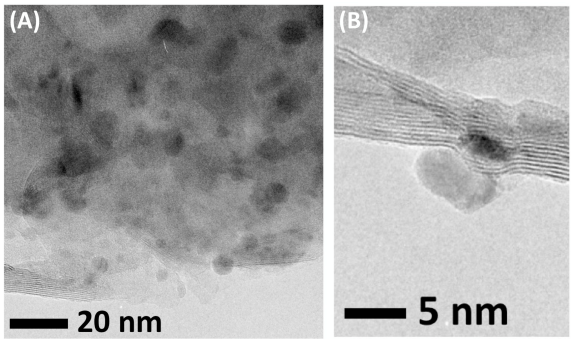


Figure 5. TEM images of $NaBH_4$-treated TNS/$Cu^{2+}$. (A) Lower and (B) higher magnification image.

**Stability of TNS/CuNP**

Generally, MNPs have low stability towards oxygen due to their small size and high surface energy; therefore, they cannot be used without protecting regents, otherwise they typically oxidise and/or aggregate. Tatsuma et al. investigated the stability of CuNPs deposited on $TiO_2$ particles.[46] They demonstrated a gradual decrease in the LSPR band, which corresponded to Cu(0) NPs observed under aerated atmosphere in the absence of a stabiliser. However, the LSPR band remained unchanged over 30 min in the presence of PVA as a stabiliser.[46] Thus, the stability of TNS/CuNP was investigated. An as-prepared TNS/CuNP film was allowed to stand in a nitrogen atmosphere and its differential extinction spectra are shown in Figure 6A. No change was observed for the extinction spectra even after >5 h under nitrogen, indicating that CuNPs within the TNS interlayers were stable. However, the extinction band corresponding to CuNP in TNS

slowly decreased when the TNS/CuNP film was allowed to stand in air and the extinction intensity was halved after 30 min, as shown in Figure 6B. PVA or poly(styrene) was spin coated on the TNS/CuNP film; however, no remarkable stabilisation of CuNPs was observed. These results suggest that oxygen molecules could easily penetrate into the interlayer space of the TNS film.

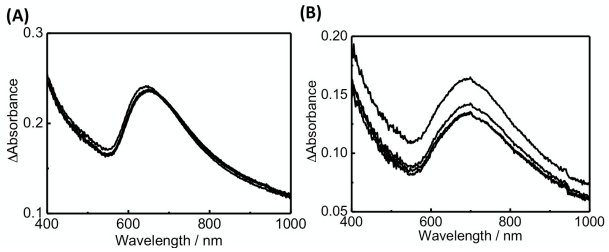


Figure 6. Differential extinction spectra of TNS/CuNP (A) upon standing in a nitrogen atmosphere for 0–5 h or (B) an aerated atmosphere for 0–30 min. Spectra were normalised by subtracting TNS/$Cu^{2+}$ as the background spectrum from the spectra obtained after $NaBH_4$ treatment.

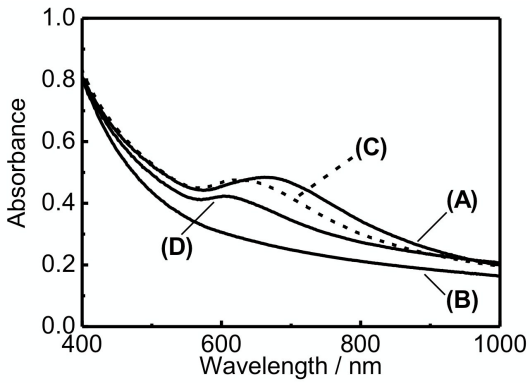


Figure 7. Extinction spectra of copper-containing TNS films: (A) as-prepared TNS/CuNP film, (B) after 24 h of treatment with oxygen, (C) after retreatment with $NaBH_4$ and (D) after nine cycles of oxygen and $NaBH_4$-treatment.

#### Recyclable Formation of CuNP within TNS

As mentioned above, upon treatment of the colourless TNS/$Cu^{2+}$ film with an aqueous solution of $NaBH_4$, a characteristic extinction peak due to the generation of CuNPs was observed at 678 nm (Figure 7A). When this film was allowed to stand for 24 h under oxygen in the dark, the extinction peak disappeared as a result of the oxidation of CuNPs (Figure 7B). Interestingly, when the oxygen-treated film was re-immersed in the aqueous $NaBH_4$ solution, the extinction peak was recovered. This suggests that once the oxidised copper species were reduced, CuNPs were reformed (Figure 7C). The extinction peak maximum of the regenerated TNS/CuNP was slightly blue-shifted (647 nm) from the initial state (Figure 7A). The origin of the blue shift is not yet clear; however, we assume that the particle shape and/or interparticle distance of CuNPs within the TNS interlayer is changed from its initial sate. This reduction and oxidation of CuNPs within TNS are repeatable, with the extinction peak persisting for at least nine cycles of oxidation in air and $NaBH_4$ treatment (Figures 7D and S10). Such recyclable properties of TNS/CuNPs are expected to demonstrate applications in cost-effective plasmonic devices and tuneable LSPR wavelengths.[54] Moreover, CuNPs as well as copper oxide NPs are expected to be applied as catalysts and co-catalysts for various chemical reactions.[33, 34, 38-40, 55] We have also synthesized other transition MNPs (Au, Ag, and Pt,) within the inorganic layered compounds in a similar way (Figure S11).[56,57] Further detail, i.e., synthesises, characterization, and optical properties of these MNP contained TNS films will be present in near future.

## Conclusions

We successfully synthesised CuNPs contained in layered semiconductor films with good transparencies. Intermediate titania nanosheet (s-TNS) films (~ 2 μm thick) exhibited relatively good transparencies. Copper ions were smoothly intercalated in the TNS layers via an $MV^{2+}$-containing TNS film as an intermediate. The colour of the copper ion-containing TNS films changed to dark metallic grey, and the characteristic extinction band was observed upon treatment with $NaBH_4$. All experimental results suggested that CuNPs form within the interlayer space of TNS films. The resultant CuNPs within the TNS interlayers gradually oxidised under aerated conditions, resulting in loss of the extinction band. This suggested that CuNPs were oxidised by oxygen in air. However, the extinction band was recovered upon treatment with $NaBH_4$. These colouration and decolouration cycles were repeatable for at least nine cycles.

## Acknowledgement

This work has been partly supported by Nippon Sheet Glass Foundation for Materials Science and Engineering, JSPS KAKENHI (Grant-in-Aid for Challenging Exploratory Research, # 50362281), and Microstructure Analysis Platform in Nanotechnology Platform Project of the Ministry of Education, Culture, Sports, Science and Technology (MEXT), Japan.

## References

1. M. Ogawa and K. Kuroda, *Chem. Rev.*, 1995, **95**, 399-438.

2. T. Yui and K. Takagi, in *Bottom-up Nanofabrication*, eds. K. Ariga and H. S. Nalwa, American Scientific Publishers, Valencia CA, 2009, vol. 5, pp. 35-90.

3. R. Sasai, T. Yui and K. Takagi, in *Encyclopedia of Nanoscience and Nanotechnology*, ed. H. S. Nalwa, American Scientific Publishers, Valencia CA, 2011, vol. 24, pp. 303-361.

4. M. Ogawa, K. Saito and M. Sohmiya, *Dalton Trans.*, 2014, **43**, 10340-10354.

5. S. Takagi, T. Shimada, M. Eguchi, T. Yui, H. Yoshida, D. A. Tryk and H. Inoue, *Langmuir*, 2002, **18**, 2265-2272.

6. T. Yui, S. Fujii, K. Matsubara, R. Sasai, H. Tachibana, H. Yoshida, K. Takagi and H. Inoue, *Langmuir*, 2013, **29**, 10705-10712.

7. K. Sato, K. Matsubara, S. Hagiwara, K. Saito, M. Yagi, S. Takagi and T. Yui, *Langmuir*, 2015, **31**, 27-31.

8. T. Tachikawa, T. Yui, M. Fujitsuka, K. Takagi and T. Majima, *Chem. Lett.*, 2005, **34**, 1522-1523.

9. T. Yui, T. Tsuchino, H. Mino, T. Kajino, S. Itoh, Y. Fukushima and K. Takagi, *Bull. Chem. Soc. Jpn.*, 2009, **82**, 914-916.

10. T. Yui, Y. Kobayashi, Y. Yamada, K. Yano, Y. Fukushima, T. Torimoto and K. Takagi, *ACS Appl. Mater. Interfaces*, 2011, **3**, 931-935.

11.T. Yui, Y. Kobayashi, Y. Yamada, T. Tsuchino, K. Yano, T. Kajino, Y. Fukushima, T. Torimoto, H. Inoue, and K. Takagi, *Phys. Chem. Chem. Phys.*, 2006, **8**, 4585-4590.

12. L. Wang and T. Sasaki, *Chem. Rev.*, 2014, **114**, 9455-9486.

13. T. Yui, Y. Mori, T. Tsuchino, T. Itoh, T. Hattori, Y. Fukushima and K. Takagi, *Chem. Mater.*, 2005, **17**, 206-211.

14. K. Akatsuka, Y. Ebina, M. Muramatsu, T. Sato, H. Hester, D. Kumaresan, R. H. Schmehl, T. Sasaki and M. Haga, *Langmuir*, 2007, **23**, 6730-6736.

15. Y. Zhou, R. Ma, Y. Ebina, K. Takada and T. Sasaki, *Chem. Mater.*, 2006, **18**, 1235-1239.

16. K. Akatsuka, G. Takanashi, Y. Ebina, M.-a. Haga and T. Sasaki, *J. Phys. Chem. C*, 2012, **116**, 12426-12433.

17. K. L. Kelly, E. Coronado, L. L. Zhao and G. C. Schatz, *J. Phys. Chem. B*, 2003, **107**, 668-677.

18. M. Rycenga, C. M. Cobley, J. Zeng, W. Li, C. H. Moran, Q. Zhang, D. Qin and Y. Xia, *Chem. Rev.*, 2011, **111**, 3669-3712.

19.N. The Binh, V. Thi Khanh Thu, N. Quang Dong, N. Thanh Dinh, N. The An and T. Thi Hue, *Advances in Natural Sciences: Nanoscience and Nanotechnology*, 2012, **3**, 025016.

20. H. Chen, L. Shao, Q. Li and J. Wang, *Chem. Soc. Rev.*, 2013, **42**, 2679-2724.

21. I. Kim, S. L. Bender, J. Hranisavljevic, L. M. Utschig, L. Huang, G. P. Wiederrecht and D. M. Tiede, *Nano Lett.*, 2011, **11**, 3091-3098.

22. D. Punj, J. de Torres, H. Rigneault and J. Wenger, *Opt. Express*, 2013, **21**, 27338-27343.

23. L. Fang, X. Wanlu, X. Qi, L. Yuxiang, C. Kaiyu, F. Xue, Z. Wei and H. Yidong, *Photonics Journal, IEEE*, 2013, **5**, 8400509-8400509.

24. Z. Bian, T. Tachikawa, P. Zhang, M. Fujitsuka, and T. Majima, *J. Am. Chem. Soc*, 2014, **136**, 458-465.

25. Z. Zheng, T. Tachikawa, and T. Majima, *Chem. Commun*, 2015, **51**, 11580-11583.

26. A. Tanaka, S. Sakaguchi, K. Hashimoto and H. Kominami, *ACS Catalysis*, 2013, **3**, 79-85.

27. X. Shi, K. Ueno, N. Takabayashi and H. Misawa, *J. Phys. Chem. C*, 2013, **117**, 2494-2499.

28. C. Gomes Silva, R. Juárez, T. Marino, R. Molinari and H. García, *J. Am. Chem. Soc.*, 2011, **133**, 595-602.

29. S. Linic, P. Christopher and D. B. Ingram, *Nat Mater*, 2011, **10**, 911-921.

30. W. Hou, W. H. Hung, P. Pavaskar, A. Goeppert, M. Aykol and S. B. Cronin, *ACS Catalysis*, 2011, **1**, 929-936.

31. W.-N. Wang, W.-J. An, B. Ramalingam, S. Mukherjee, D. M. Niedzwiedzki, S. Gangopadhyay and P. Biswas, *J. Am. Chem. Soc.*, 2012, **134**, 11276-11281.

32. V. Subramanian, E. E. Wolf and P. V. Kamat, *Langmuir*, 2003, **19**, 469-474.

33. K. Lalitha, G. Sadanandam, V. D. Kumari, M. Subrahmanyam, B. Sreedhar and N. Y. Hebalkar, *J. Phys. Chem. C*, 2010, **114**, 22181-22189.

34. M. Y. Kang, H. J. Yun, S. Yu, W. Kim, N. D. Kim and J. Yi, *J. Mol. Catal. A: Chem.*, 2013, **368–369**, 72-77.

35. N. Sakai, T. Sasaki, K. Matsubara and T. Tatsuma, *J. Mater. Chem.*, 2010, **20**, 4371-4378.

36. M. Eguchi, M. Ito and T.-a. Ishibashi, *Chem. Lett.*, 2014, **43**, 140-142.

37. S. Adireddy, T. Rostamzadeh, C. E. Carbo and J. B. Wiley, *Langmuir*, 2015, **31**, 480-485.

38. C.-C. Yang, Y.-H. Yu, B. van der Linden, J. C. S. Wu and G. Mul, *J. Am. Chem. Soc.*, 2010, **132**, 8398-8406.

39. C. W. Li, J. Ciston and M. W. Kanan, *Nature*, 2014, **508**, 504-507.

40.E. Pastor, F. M. Pesci, A. Reynal, A. D. Handoko, M. Guo, X. An, A. J. Cowan, D. R. Klug, J. R. Durrant and J. Tang, *Phys. Chem. Chem. Phys.*, 2014, **16**, 5922-5926.

41. T. Sasaki, Y. Komatsu and Y. Fujiki, *J. Chem. Soc., Chem. Commun.*, 1991, 817-818.

42. T. Sasaki and M. Watanabe, *J. Am. Chem. Soc.*, 1998, **120**, 4682-4689.

43. T. Hattori, Z. Tong, Y. Kasuga, Y. Sugito, T. Yui and K. Takagi, *Res. Chem. Intermed.*, 2006, **32**, 653-669.

44. R. D. Shannon, *Acta Crystallogr.*, 1976, **A32**, 751.

45. E. Kazuma, T. Yamaguchi, N. Sakai and T. Tatsuma, *Nanoscale*, 2011, **3**, 3641-3645.

46. T. Yamaguchi, E. Kazuma, N. Sakai and T. Tatsuma, *Chem. Lett.*, 2012, **41**, 1340-1342.

47.X. Lu, M. Rycenga, S. E. Skrabalak, B. Wiley and Y. Xia, *Annu. Rev. Phys. Chem.*, 2009, **60**, 167-192.

48. E. Hutter and J. H. Fendler, *Adv. Mater.*, 2004, **16**, 1685-1706.

49.S. Underwood and P. Mulvaney, *Langmuir*, 1994, **10**, 3427-3430.

50. S. K. Ghosh and T. Pal, *Chem. Rev.*, 2007, **107**, 4797-4862.

51. I. E. Grey, C. Li, I. C. Madsen and J. A. Watts, *J. Solid State Chem.*, 1987, **66**, 7-19.

52. T. Sasaki, Y. Ebina, Y. Kitami, M. Watanabe and T. Oikawa, *J. Phys. Chem. B*, 2001, **105**, 6116-6121.

53. V. Hayez, A. Franquet, A. Hubin and H. Terryn, *Surf. Interface Anal.*, 2004, **36**, 876-879.

54. H. Cheng, X. Qian, Y. Kuwahara, K. Mori and H. Yamashita, *Adv. Mater.*, 2015, **27**, 4616-4621.

55. J. Zhang, W. Liu, X. Wang, X. Wang, B. Hu and H. Liu, *Appl. Surf. Sci.*, 2013, **282**, 84-91.

56. K. Sasaki, S. Kawamura, F. Takagi, K. Saito, M. Yagi, and T. Yui, *Abstract of XXV IUPAC Symposium on Photochemistry*, 2014, P279.

57. T. Yui, S. Kawamura, K. Sasaki, F. Takagi, K. Saito, M. Yagi, W. Norimatsu, and R. Sasai, *Abstract of Annual Meeting on Photochemistry 2015*, 2015, 3D12.

Graphical Abstract Caption

We report the first *in situ* synthesis of copper nanoparticles (CuNPs) within the interlayer space of inorganic layered semiconductor (titania nanosheet; TNS) transparent films.

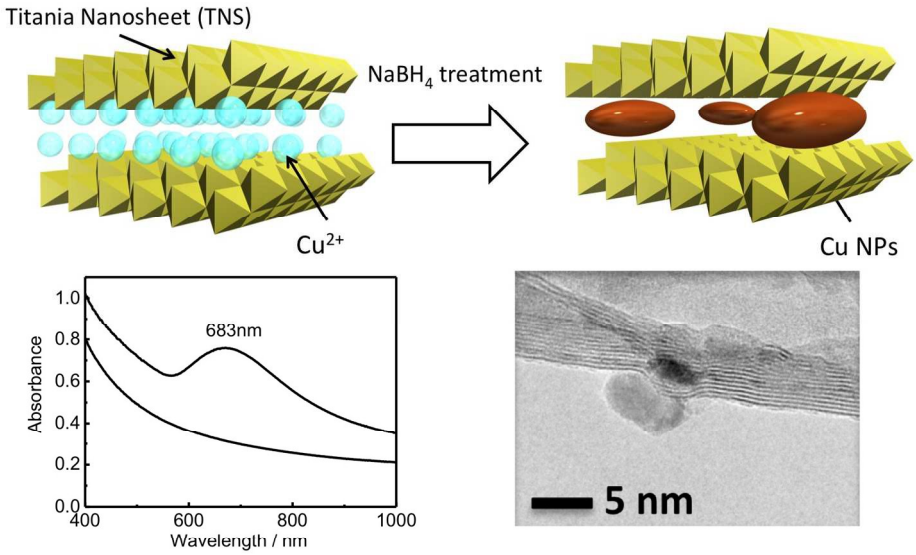


635x476mm (72 x 72 DPI)